

# Implementation of a Carrier Frequency Recovery Loop for MIMO-CDMA Systems

Hamid Eslami, Ahmed M. Eltawil

University of California, Irvine  
[heslami](mailto:heslami@uci.edu), [aeltawil](mailto:aeltawil@uci.edu) @uci.edu

**Abstract:** This paper presents simulation and implementation results of a fine frequency tracking loop optimized for Multiple-Input Multiple-Output (MIMO), Code Division Multiple Access (CDMA) receivers. The proposed tracking loop exploits spatial diversity and multi-threshold recovery schemes to improve the loop's robustness, convergence time and accuracy. Comprehensive simulation results in a frequency-selective Rayleigh fading channel are presented, as well as implementation results using a 0.18 um CMOS technology.

**Index Terms:** MIMO-CDMA, carrier frequency recovery, Rayleigh fading.

## I. INTRODUCTION

In MIMO-CDMA systems not only are all users sharing a common communication medium at the same time, but through MIMO techniques each user transmits multiple streams of data thus deteriorating the overall interference experienced by other users in the cell. In such systems the robustness and performance of timing and frequency recovery circuits are crucial.

In this paper, we will focus on frequency recovery in MIMO-CDMA systems where due to intrinsic imperfections in practical devices there are potential mismatches between transmit and receive systems that need to be alleviated for fast reliable data transmission. Crystal frequency offsets are a significant source of such mismatches and have to be compensated at the receiver end. Commercially available crystals can have up to 10 PPM frequency accuracy leading to  $\pm 20$  KHz offset at a carrier frequency of 2 GHz<sup>1</sup>. Typically a two step approach is used to compensate for such offset. Initially, a coarse FFT is taken to bring the offset down to  $\pm 2.0$  KHz at which point a fine frequency tracking loop is used to converge to within  $\pm 200$  Hz.

Carrier frequency estimation (using FFT techniques) has been well studied in literature and established algorithms are now typically used to achieve ( $\pm 2.0$  KHz or 1 PPM) accuracy [1]. Focusing on the fine frequency recovery effort ( $\pm 200$  Hz accuracy or  $\pm 0.1$  PPM), we are proposing a robust tracking scheme for frequency recovery in MIMO-CDMA systems. The circuit exploits diversity in the received pilot symbols to improve both tracking resolution as well as convergence time.

The paper is organized as follows: section II discusses the architecture of a MIMO-CDMA system. Section III presents analytic and block diagram description of the proposed scheme. In section IV simulation results are presented, while section V describes the VLSI implementation. Finally, section VI concludes the paper.

## II. SYSTEM ARCHITECTURE

Figure 1 depicts the block diagram of a MIMO-CDMA system for one antenna array at either ends. This could be extended to multiple transmitter arrays with different CDMA patterns as well as multiple receiver arrays with their correspondent pattern for CDMA decoder. Data for each user is first mapped on a unique pseudo-noise (PN) sequence, then up converted to radio frequency  $f_c$  and finally passed through the transmit antenna array. The CDMA sequence is of length  $F$  and has raised-cosine pulse shaping, leading to a base-band waveform expressed as follows:

$$C^i(t) = \sum_{j=1}^k a_j^i P(t - jT_c) \quad (1)$$

where superscript  $i$  is the number of user,  $a_j$  indicates the status of  $j^{th}$  chip in CDMA sequence and  $P(t)$  is raised-cosine pulse as mentioned before. The out going RF signal therefore, has the following format:

$$D^i(t) = A^i \left( \sum_{k=1}^{DL} d_k C^i(t) \right) e^{j2\pi f_c t} \quad (2)$$

where  $A^i$ ,  $DL$ ,  $d_k$  are respectively the amplitude, data length and the  $k^{th}$  bit of data stream corresponding to the  $i^{th}$  user.

This data then is sent through the air via multiple antenna elements in MIMO-CDMA systems. Depending on the structure of the channel that the signal travels through

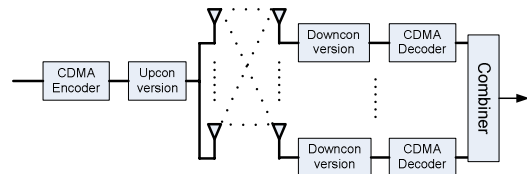


Figure 1, MIMO-CDMA system block diagram

<sup>1</sup> The values quoted are pertinent to a 3GPP WCDMA system operating in the 2 GHz band.

3GPP Test Case	Speed (Km/h)	Multi-path Profile	
		Delay(ns)	Mean Power(dB)
1	3	Flat Fading	
2	3	0	0
		976	-10
3	3	0	0
		976	0
		20000	0
4	120	0	0
		1040	-3
		2084	-6
		3124	-9

Table 1, 3GPP WCDMA multipath profiles

different fading profiles could be defined for different channels. In this study, we considered four different Rayleigh fading channels as shown in table 1. These cases are standardized test cases as defined in the 3GPP standard [2].

The channel is considered as a filter with the following impulse response:

$$h(t) = \sum_{i=1}^{MP} \alpha_i e^{j\theta_i} \delta(t - \tau_i) \quad (3)$$

where  $\alpha_i$  is a complex Gaussian random variable,  $\theta_i$  is a uniform random variable and  $MP$  and  $\tau_i$  are number of multipath and its corresponding delay from multi-path profile. Also  $\alpha_i$  and  $\theta_i$  are updated at the channel coherence time rate.

At the receive end, the received signal is down converted to either base band or IF and processed through a detection phase. A block diagram of the detection phase structure of receiver is depicted in Figure 2. The incoming signal is sampled at twice the Nyquist rate ( $4x$ ) and then adjusted by the frequency recovery tracking loop output which will be discussed in details further on. The whole idea is to compensate for the mismatch in the crystal that generates the master clock signal ( $f_m$ ) in the receiver. This compensation is accomplished by estimating the offset through the frequency unit and applying it to the incoming signal prior to any process. The signal then undergoes CDMA processing within a processing unit (PU) in which the received signal is correlated with a locally generated PN code and the result is used to extract transmitted data as well as to feed the tracking loop. Within a PU each multipath component is treated as a separate entity independent of which actual receive antenna it belongs to. This separation facilitates spatial and temporal processing further down the chain to exploit diversity in the received pilot symbols for frequency recovery. The frequency unit is therefore benefiting from both spatial (antenna) and temporal (RAKE processing) diversity, which directly translates to improved accuracy and convergence speed. The assumption made here is that the pilot symbols received on

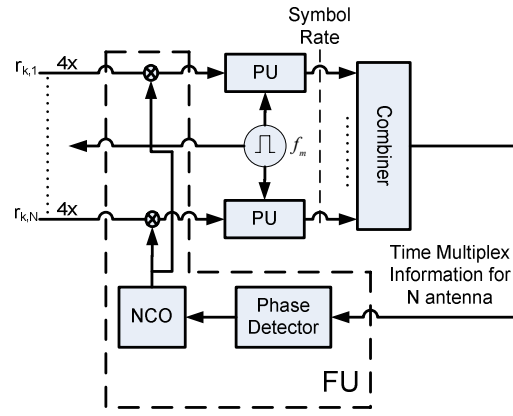


Figure 2, multiple antenna element receiver structure

both antennas are identical. Finally at the frequency unit (FU), adjustment factors are computed based on correlation results. The FU comprises of a phase detection (PD) that computes the amplitude and phase of the correction factors and a numerically controlled oscillator (NCO) coupled with a direct digital frequency synthesizer (DDFS) [3] that are used to generate the compensation frequency based on the PD's output.

### III. TRACKING LOOP

Frequency offset at the receiver end leads to an imperfect down conversion process which causes a drift in the correlation results performed on the pilot. In the other words, the PU output rotates in the complex plane proportional to its relevant frequency offset. This concept is depicted in Figure 3 where correlation results are illustrated for two different frequency offsets  $f_{offset1} > f_{offset2}$  corresponding to  $\theta_1$  and  $\theta_2$  where  $f_{offset1} > f_{offset2}$ . To compensate for this frequency offset the incoming waveform is pre-rotated in order to mitigate the crystal frequency offset in the subsequent stages. Equivalently, the incoming waveform is multiplied by an exponential term with negative phase (pre-rotation) compensating for the intrinsic frequency offset caused by the mismatches. The system implementing this scheme is depicted in Figure 4. With knowledge of the multi-path profile, a controller selects the pilot symbol of the strongest multi-path from each antenna. This pilot symbol is correlated over 512 successive

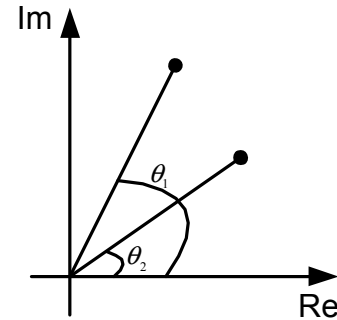


Figure 3, Pilot positions for two frequency offsets

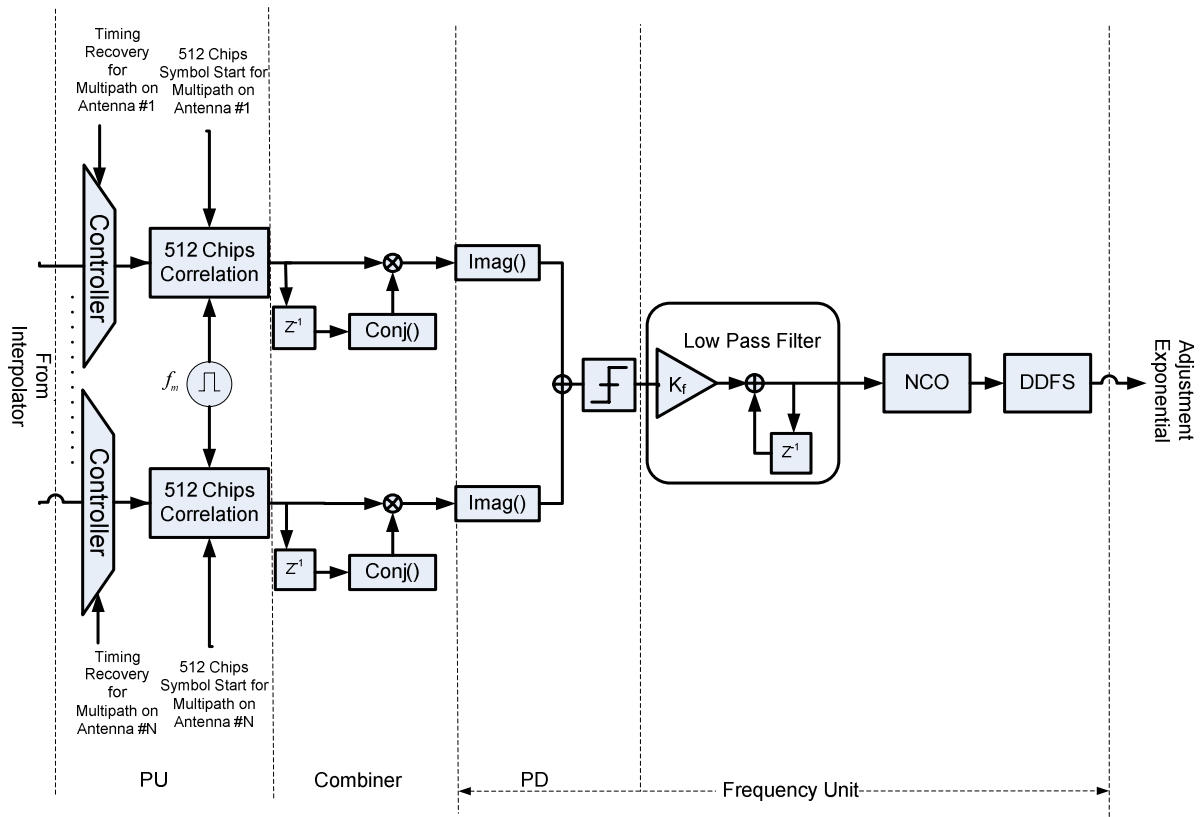


Figure 4, Frequency recovery tracking loop

chips in the PU. A combining unit then measures the phase difference of two successive spreading blocks, simply by multiplying the correlation result of the current symbol with the conjugate of that of the previous symbol as follows:

$$y_s(n) = x_s(n) * \text{conj}(x_s(n-1)) \quad (4)$$

where  $y_s(n)$  is the combiner's output of antenna element number  $s$  and  $x_s(n)$  is the same antenna's correlation output for the  $n^{\text{th}}$  bit. To let the frequency offset reflect in  $y_s(n)$  and cancel out the signal affect, a training sequence transmits through channel that leaves  $y_s(n)$  to be a function of crystal offset distorted by noise and fading.  $y_s(n)$  therefore could be considered to have the following form:

$$y_s = A e^{j\omega} \quad (5)$$

The imaginary value of  $y_s(n)$  is a measure of the frequency offset occurred in the pilot symbol. This can be easily observed from Figure 3 where the frequency offset results in a phase offset as shown in the figure. The phase detector in the FU operates based on this principle and determines whether the recovery pilot signal has to be increased in frequency or decreased (both in absolute value). Negative-phased  $y_s(n)$ , i.e. negative imaginary part, corresponding to  $\theta_n < \theta_{n-1}$  states that recovery frequency has to be increased and vice versa.

However, due to noise and fading in the channel, false-alarms could occur, meaning that the channel artifacts displace the

correlation results to the point that the PD makes an erroneous decision. Diversity techniques help to alleviate this by averaging over more than one PD's output. This can be implemented as follows:

$$FRF = K \cdot \text{sign}(\text{Im} \text{ag}(\sum_{i=1}^N x_i(n) \cdot x_i^*(n-1))) \quad (6)$$

where  $K$  is the proportionality factor and  $N$  is the number of receive antenna elements. Frequency refinement factor (FRF) expression could be a more complex function of correlation outputs to make the convergence much faster. For example, instead of one step sign function we could use multiple step sign function (multi-threshold scheme) which significantly affects the convergence time. In the following sections, we will investigate these design tradeoffs. The remaining parts of FU are a low pass filter with gain  $K_f$  feeding the NCO with a frequency input word (FIW) that drives a direct digital frequency synthesizer (DDFS) to generate the corresponding sine/cosine values and close the loop.

#### IV. SIMULATION RESULTS

##### A. Performance and spatial diversity

Simulations are performed based on a pilot CDMA code length of 512 and  $SNR = -10\text{dB}$  prior to de-spreading unless otherwise stated. The maximum crystal frequency offset is set to be 1500 Hz (post coarse FFT) and a 1x2 SIMO system is chosen as a test case.

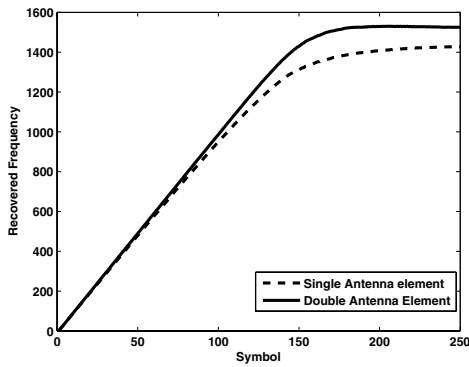


Figure 5, Mean performance of tracking loop  
For single and double antenna elements

Figure 5 illustrates the impact of diversity processing on the loop performance. The plot depicts the average performance of the loop over 1000 channel realizations based on Rayleigh fading channel case number 2 (refer to Table 1). Proportionality factor is set to be 10 Hz for both cases. From the figure, one can identify that the dual antenna system exhibits superior performance in both accuracy and transition time. The dual antenna system converges to 98.5 percent of maximum frequency offset (1500 in our case) while a single antenna system reaches up to 95.1 percent under the same conditions. It is necessary to mention that in an AWGN channel the frequency recovery loop recovers up to maximum frequency offset within  $\pm$  FRF Hz as expected, furthermore the gains in the flat fading condition are expected to be even more pronounced.

To further quantify the gains associated with diversity a CDF of rising time (10 to 90 percent of maximum frequency offset) normalized in symbols is plotted in Figure 6. In both curves  $K$  is 10 Hz and kept constant through out the recovery process.

#### B. Performance and multi-threshold schemes

As mentioned earlier, pilot analysis shows a major drift in correlation's pilot position at the beginning of the recovery process. To speed up the procedure, a multi-threshold recovery scheme could be deployed as follows: Proportionality factor,  $K$  is set to a large value therefore frequency recovery starts with large steps. When correlation's pilot reaches a predefined threshold,  $K$  changes to a smaller value making  $FRF$  smaller. In this way, convergence time reduces dramatically and convergence accuracy improves since the loop takes finer steps in the second stage. Figure 7 illustrates this improvement where the loop's performance is plotted for three different scenarios based on multipath profile case 3. It can be seen that double-threshold recovery schemes converges faster and more accurately than single-level recovery scheme. In all three cases, performance is averaged over 1000 channel realizations.

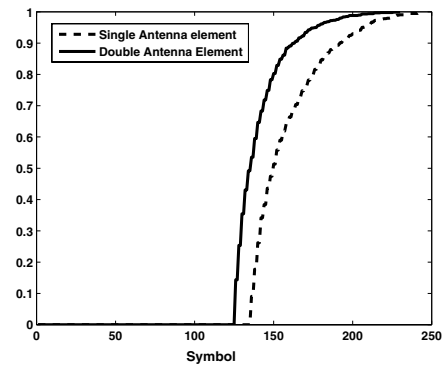


Figure 6, CDFs of rising time comparing single  
and double antenna elements

To illustrate how multi-threshold recovery scheme affects the statistics of the loop, the CDFs of rising time for 3GPP test case 1, 3, 4 are depicted in Figure 8. One can notice a drastic improvement in double-thresholds cases where on average the convergence time is improved by a factor of 2x (55 symbols at  $p = 0.5$ ). The benefit of fast convergence is in addition to the improved accuracy as shown in Figure 7.

It can be seen in Figure 8 that for channels with higher scattering i.e. 3GPP test case 3 and 4, the loop performs better and that is because the strongest multipath component is chosen from each antenna element and therefore channels with more multipath components on average due to higher signal to noise ratio (SNR) perform better.

#### C. Performance versus SNR

The extent to which SNR affects the performance of the loop is illustrated in Figure 9 where mean convergence time (10 to 90 percent of maximum frequency offset) normalized in symbols is depicted versus SNR.

Figure 9 (a) shows the mean convergence time versus SNR of a flat fading channel for single-antenna single-threshold configuration and double-antenna, double-threshold, configuration with selection combining (SC) diversity technique. Figure 9 (a) illustrates that a significant improvement

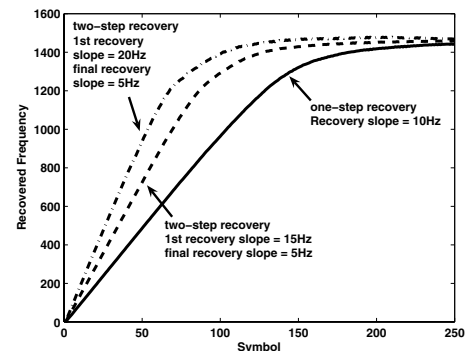


Figure 7, Mean recovering time (normalized in symbols) for single and two-step recovery scheme

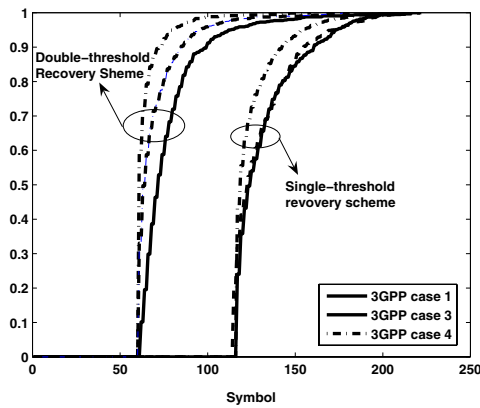


Figure 8, CDFs of rising time comparing single versus double threshold recovery schemes

is achieved (almost 3dB gain in convergence time) for SNR=-10dB when double-antenna double-threshold configuration is deployed.

Figure 9 (b) depicts the loop performance versus SNR for 3GPP case 4 (high scattering). Again a drastic improvement is attained exploiting double-antenna double-threshold configuration with selection combining diversity. For comparative analysis purposes, the results are extended to include utilizing equal gain combining (EGC) at the input of the system. From the figure, it is clear that the differential gain between utilizing EGC versus simpler selection diversity is not exceptionally large.

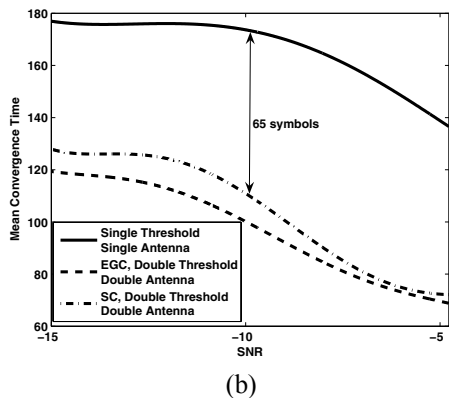
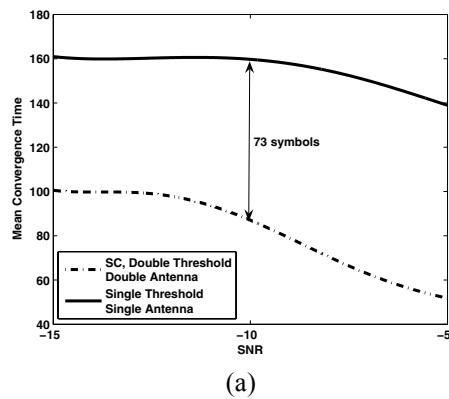


Figure 9, Mean convergence time versus SNR for flat fading channel (a) and 3GPP case 4 (b)

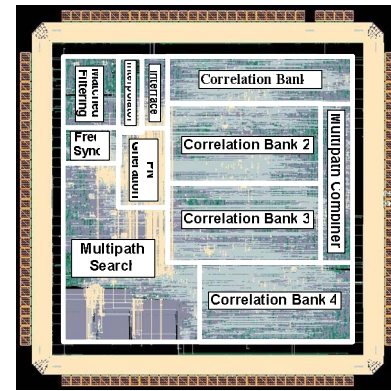


Figure 10 Modem die

## V. VLSI IMPLEMENTATION

The simulation results presented in the past sections led to the selection of a dual threshold, selection based frequency recovery unit to be fabricated as part of a larger CDMA modem that can demodulate up to 20 multipath. The technology used is 0.18 $\mu$ m CMOS with 1 poly layer and 6 metal layers. The supply voltage for the core is 1.8v with 3.3v for the pads. The frequency range of operation is 64-107MHz.

The frequency unit occupies an area of 29,000 $\mu$ m<sup>2</sup> which is equivalent to 940 two input NAND gates. Figure 10 depicts a die photo of the fabricated chip with the location of different blocks including the frequency synchronization unit identified. Running at a nominal clock frequency of 80 MHz the entire chip core consumes 22 mw of which 0.3 mw are used by the frequency unit.

## VI. CONCLUSION

In this paper, we proposed a novel method for carrier frequency recovery in MIMO-CDMA systems. The proposed scheme was shown to be accurate, robust and very easy to implement which makes it suitable for many CDMA applications.

## REFERNECES

- [1] W.K.M. Ahmed, P.J. McLane, "A simple method for coarse frequency acquisition through FFT," in *proceedings of IEEE Vehicular Technology Conference*, vol.1, pp.297 - 301, June 1994.
- [2] 3GPP TS 25.101 V3.11.0, "UE Radio Transmission and Reception (FDD)", June 2002.
- [3] A. M. Eltawil and B. Daneshrad, "Interpolation based direct digital frequency synthesis for wireless communications," in *proceedings of the IEEE Wireless Communications and Networking Conference (WCNC)*, vol.1, pp.73-7, March 2002.